Three-dimensional nuclear organization in Arabidopsis thaliana

Frederic Pontvianne, Stefan Grob

Three-dimensional nuclear organization in *Arabidopsis thaliana*

Frédéric Pontvianne[1,2*] and Stefan Grob[3*]

[1]UPVD, LGDP UMR5096, Université de Perpignan, Perpignan, France

[2]CNRS, LGDP UMR5096, Université de Perpignan, Perpignan, France

[3]Institute of Plant and Microbial Biology, University of Zurich, Zurich, Switzerland

*Correspondence to: sgrob@botinst.uzh.ch ; fpontvia@univ-perp.fr

Abstract

In recent years, the study of plant three-dimensional nuclear architecture received increasing attention. Enabled by technological advances, our knowledge on nuclear architecture has greatly increased and we can now access large data sets describing its manifold aspects. The principles of nuclear organization in plants do not significantly differ from those that in animals. Plant nuclear organization comprises various scales, ranging from gene loops to topologically associating domains to nuclear compartmentalization. However, whether plant three-dimensional chromosomal features also exert similar functions as in animals is less clear. This review discusses recent advances in the fields of three-dimensional chromosome folding and nuclear compartmentalization and describes a novel silencing mechanism, which is closely linked to nuclear architecture.

Keywords:

Arabidopsis, Chromosome Conformation Capture, Hi-C, Nuclear Compartments

Introduction

The nucleus is the core-organelle of eukaryotic cells and provides manifold services. The nuclear genome is responsible for storage, amplification, release, and integration of vital information. Most cellular responses to external cues rely on nuclear responses, including the up- or down-regulation of relevant genes and non-coding RNAs. The highly complex organization of genomes allows to provide these variable and sometimes conflicting services simultaneously. Differential genome regulation can be achieved as genomes are organized on several levels: 1) the linear DNA sequence, which contains the genetic information and regulatory sequences, 2) the chromatin landscape that comprises chemical modifications of the DNA and DNA-associated proteins, 3) the three-dimensional (3D) genome folding, and 4) the chromatin's absolute 3D-position within the nucleus.

The genome of the model plant *Arabidopsis thaliana* (L.) Heynh. belongs to the best studied ones in plants and information for all four levels is available, however, to different extent. Whereas we have access to a nearly complete assembly of the linear DNA sequence (Lamesch et al. 2012) and in-depth epigenomic profiling of cytosine methylation and numerous histone modifications (e.g. Lister et al. 2008; Stroud et al. 2014; Zhang et al. 2006), much less is known on 3D genome folding and nuclear compartmentalization. Using cytological approaches, 3D aspects of plant genomes have been studied for a many years, revealing the existence of specific chromosome configurations in cereals (Santos and Shaw 2004), chromosome territories, and epigenetic compartmentalization into hetero- and euchromatin in mosses (Heitz 1928) and higher plants (Fransz et al. 2002). In *A. thaliana*, heterochromatin can be cytologically detected as chromocenters (Fransz et al. 2002) that likely correspond to the constitutive heterochromatin of pericentromeres. In addition to observing these basic 3D chromosome organization units, microscopy-based approaches also allowed to study the responses of the 3D genome to ectopic stimuli, such as biotic stress and light (Barneche et al. 2014; Kaiserli et al. 2015; Pavet et al. 2006; Pecinka et al. 2010; Tessadori et al. 2007). However, despite steadily improving resolution of microscopy (Szabo et al. 2018), cytological approaches can still not be employed to monitor single transcriptional units, such as genes of several kilo bases (kb), a dimension, which is likely relevant for 3D organization of chromatin. In recent years, the field made a step forward and our knowledge on plant 3D nuclear architecture has significantly increased (Doğan and Liu 2018; Sotelo-Silveira et al. 2018; Stam et al. 2019). Novel technologies enabled this progress and increased resolution to study

nuclear architecture was achieved by employing molecular techniques, such as Chromosome Conformation Capture (3C) (Dekker et al. 2002) technologies that reveal 3D contact frequencies between chromatin fragments of typically less than 10 kilobases in size. It is worth noting that certain discrepancies between cytological observation and 3C results can arise, likely as - in contrast to microscopy - 3C technologies are usually employed on large pools of cells (Grob and Grossniklaus 2017) and, thus, reveal averaged 3D-folding principles. In recent years, 3C technologies definitely arrived in the plant field and especially the genome-wide derivative of 3C, Hi-C, has been conducted in many different plant species, providing 3D contact maps throughout the plant kingdom (Dong et al. 2017; Hu et al. 2019b, 2019c; Jibran et al. 2018; Liu et al. 2017; Maccaferri et al. 2019; Mascher et al. 2017; Moissiard et al. 2012; Raymond et al. 2018; Shi et al. 2019; VanBuren et al. 2018; Zhang et al. 2018; Zhu et al. 2017). Interestingly, these data sets also include 3D-contact maps of non-canonical genomes, such as those of hybrids and allotetraploids (Maccaferri et al. 2019; Wang et al. 2018; Zhu et al. 2017). Despite the large efforts to generate data relevant for 3D genome maps, many of them await in-depth analysis, as a majority of Hi-C experiments were performed to enable *de novo* assembly of genomes and limited effort has been invested to study 3D genome architecture in the respective species.

Principles of plant genome folding.

Eukaryotic 3D genome organization comprised several scales, ranging from large chromosomal domains of several megabases (Mb) to genomic loops, spanning less than one kb. How and whether the different scales depend on each other is still a matter of debate. At the largest scale and in accordance to cytological observation, Hi-C data can be used to describe chromosome territories, which correspond to distinct volumes occupied by single chromosomes within the nucleus (Cremer and Cremer 2001). Furthermore, Hi-C is also suitable to describe certain chromosome configurations that were previously cytologically defined: In *A. thaliana*, frequent contacts between telomeres and centromeres can be readily observed, which are hallmarks of the rosette configuration (Fransz et al. 2002; Grob et al. 2014). Interestingly, other cytological features of the rosette configuration (Fransz et al. 2002), such as frequent and periodic contacts between chromosome arms and pericentromeres could not be confirmed by Hi-C (Grob and Grossniklaus 2017). The apparent discrepancy is not easily explained and does not necessarily indicate a weakness of either 3C or cytological techniques. The rosette loop anchors may not be well defined, leading to signal dilution in Hi-

C data, whereas these loops may still be readily observable by whole chromosome painting (Fransz et al. 2002). In the Rabl-configuration centromeres and telomeres are located to opposite poles of the nucleus and the two chromosome arms are placed in parallel to each other (Fang and Spector 2005). This Rabl-configuration specific feature, can be observed in Hi-C maps by increased contact frequencies perpendicular to the diagonal of the maize Hi-C maps (Dong et al., 2019). In non-rabl configured genomes with metacentric chromosomes, two distinct chromosome-arm-territories are detected, manifested by depleted contact frequencies between fragments located on either side of the centromere. Hence, the centromere can act as 3D boundary (Grob et al. 2013; Pecinka et al. 2004).

Another organizational feature, which also occurs at a Mb-scale are A- and B-compartments, which highly correlate to the epigenetic landscape (Grob et al. 2014; Lieberman-Aiden et al. 2009). Characteristic for A- and B-compartments are enriched contact frequencies among chromosomal regions with similar epigenetic features throughout the genome. Generally, A-compartments are associated with an active epigenetic state, whereas B-compartments include chromosomal regions of repressed epigenetic state (Grob et al. 2014; Lieberman-Aiden et al. 2009). However, A- and B- compartments cannot be clearly associated to biologically relevant organizational features. They are determined by the algebraic sign of the Eigenvector resulting from a principal component analysis (PCA) and the PCA highly depends on the data fed into the analysis. A- and B- compartments of entire and fully assembled chromosomes usually correspond to the euchromatin of chromosome arms and pericentromeric heterochromatin, respectively. As these compartments were identified well before the onset of 3C technologies [5], one may argue that their identification by Hi-C does not bring along a major advance in our understanding of 3D genome architecture. However, the two compartments may describe very different chromosomal region when only Hi-C data from chromosome arms are fed into the analysis, in which case previously undetected sub-compartmentalization of chromosome arms can be detected. In *A. thaliana*, these compartments are referred to as loose and closed structural domains (LSDs and CSDs) and correlate to active and partially repressed euchromatin, respectively (Grob et al. 2014). Thus, A- and B- compartments are not strictly biologically relevant terms and they do not only rely on the Hi-C data fed into the PCA but also heavily on the assembly status of the genome in question. Many genome assemblies do not include repetitive regions, which are covering large sections of pericentromeric heterochromatin (dos Santos et al. 2015), thus the resulting A-

and B- compartments in species with incomplete genome assemblies may rather resemble *A. thaliana* LSDs and CSDs of euchromatic chromosome arms.

Chromosome arms are typically further subdivided into topologically associating domains (TADs). A TAD comprises neighboring chromosomal regions that exhibit high 3D contact frequencies among each other but depleted contacts with other chromosomal regions in close proximity (Bonev and Cavalli 2016; Sexton et al. 2012). In a less technical view, TADs can be perceived as a chain of pearls of different sizes, being 3D structures that are clearly delineated from each other. Interestingly, unlike in most other species analyzed by Hi-C (Bonev and Cavalli 2016), TADs are not prominent features of *A. thaliana* Hi-C maps (Feng et al. 2014; Grob et al. 2014; Moissiard et al. 2012). However, the apparent absence of TADs in *A. thaliana* cannot be extrapolated to other plant species, as since the first Hi-C experiments conducted in *A. thaliana*, TADs have been detected in many other plant species (Dong et al. 2017; Hu et al. 2019b, 2019c; Jibran et al. 2018; Liu et al. 2017; Maccaferri et al. 2019; Mascher et al. 2017; Moissiard et al. 2012; Raymond et al. 2018; Shi et al. 2019; VanBuren et al. 2018; Zhang et al. 2018; Zhu et al. 2017). *A. thaliana* may even exhibit a rather unusual 3D chromosomal architecture, as many Hi-C maps from plants (including both, mono- and dicots) resemble those acquired in animals.

Despite these phenotypic similarities to animal 3D chromosome organization, plant TADs likely differ from animal TADs in molecular and possibly functional aspects. In animals, TAD borders are enriched in CCCTC-binding factor (CTCF) and previous experiments have shown that both the presence and orientation of CTCF binding sites are essential for TAD formation (Guo et al. 2015; Phillips and Corces 2009). In plants, CTCF homologues have not been identified to date, indicating that it is not *per se* required for 3D boundary formation. This hypothesis is in line with previous studies showing that bio-physical processes independent of specific insulator proteins may be sufficient to form 3D chromosomal structures, such as TADs (Alipour and Marko 2012; Cook and Marenduzzo 2018; Rada-Iglesias et al. 2018; Strom et al. 2017). In animals, CTCF exerts its insulating function in association with cohesin (Schwarzer et al. 2017), which is thought to form a ring-like structure and thereby tethering contacting chromosomal regions (Rowley and Corces 2018; Szabo et al. 2019). According to the currently most favored model – the “loop extrusion model” (Sanborn et al. 2015) –, loop and TAD formation is a dynamic process, which requires a fine-tuned balance of both CTCF binding and cohesin activity (Rowley and Corces 2018; Szabo et al. 2019). In contrast to CTCF, cohesin

homologs can be found in plants (Schubert et al. 2009) and appear to play a vital role. In *A. thaliana*, microscopical observation revealed severe phenotypes affecting chromosomal architecture in cohesin-complex mutants (Schubert et al. 2009). To date, no Hi-C data sets describing cohesin mutants have been published in plants.

On a global scale, plant and animal TADs share similar characteristics, such as active transcription and enrichment of active epigenetic marks at TAD borders (Liu et al. 2017). However, they may differ on a functional level: animal TADs appear to mainly function in transcriptional control of the within located genes (Rowley and Corces 2018; Szabo et al. 2019). The compartmentalization within single TADs may ensure that promoters are in contact with relevant enhancer elements and also protects these promoters from ectopic contacts with distant enhancers, which may lead to deleterious mis-expression of genes (Szabo et al. 2019). Plant TADs may exert different – yet to date unknown – function (Dong et al. 2017; Stam et al. 2019), as regulatory contacts between putative enhancer and promoter elements occur across TAD boundaries (Dong et al. 2017).

The wide-spread occurrence of TADs and their apparent absence in *A. thaliana* has led to speculations on additional factors enabling TAD formation. One of these factors may be genome size: comparative analysis between several plant species (Dong et al. 2017; Stam et al. 2019) has shown that in species with genomes smaller than 400 Mb, prominent TADs cannot be detected. However, whether genome size really affects TAD formation can be debated. Hi-C data sets for plant species with genomes of less than 400 Mb are scarce and these species are highly related (*Arabidopsis thaliana* and *Arabidopsis lyrata* (Zhu et al. 2017)). Furthermore, *Drosophila melanogaster* has a genome size (ca. 180 Mb (dos Santos et al. 2015)) comparable to *A. thaliana* and clear delineation into TADs can be observed. Features of *Drosophila* 3D genome architecture may however hint another explanation for the absence of TADs in *A. thaliana*. *Drosophila* TADs can be categorized by their epigenetic landscape and significant changes in epigenetic characteristics of chromatin coincides with borders between TADs (Sexton and Cavalli 2015). Intriguingly, the *A. thaliana* epigenetic landscape only rarely shows abrupt changes. Thus, the rather uniform distribution of epigenetic marks along *A. thaliana* chromosome arms may explain why TADs cannot be found in these chromosomal regions (Rowley et al. 2017; Stam et al. 2019). In support of this, TAD border-like 3D delineation can be observed in regions where the epigenetic landscape abruptly changes. The *A. thaliana knob hk4s* clearly shows TAD-like features (Grob et al. 2013, 2014) and boundaries

between pericentromeres and euchromatic chromosome arms are clearly detectable in *A. thaliana* Hi-C data sets.

Despite the large efforts done in recent years, we still lack functional insight into large-scale structures, such as chromosome territories, A/B compartments, and TADs, and their relevance for nuclear processes remains to be elucidated. Possibly, they are not suited to be investigated in an isolated fashion, but their occurrence should be rather put into context to the absolute 3D localization of chromosomes within nuclei.

Putting back the chromatin domains in the nuclear context

Taking into account the context of a TAD is important to understand its biology. TADs can indeed associate or be in close proximity with different nuclear compartments such as the nucleolus, nuclear speckles, Cajal bodies, nuclear pore complex, or the nuclear periphery. The nuclear periphery occupies a large volume in the nucleus. As a result, a large part of the genome is associated with the nuclear periphery. At least in *A. thaliana,* repeated sequences present in the centromeric and the pericentromeric regions, as well as ribosomal RNA genes repeats, are organized as chromocenters (CCs) (Fransz et al. 2002). Analyses of their relative distribution revealed their preferential association with the nuclear periphery, displaying a repulsive-like spatial distribution (Andrey et al. 2010). In metazoans, large portions of the genome are maintained at the nuclear periphery by a network of fibers composed largely of nuclear lamins. These domains were called LADs, for lamina-associated chromatin domains (Guelen et al. 2008; Pickersgill et al. 2006; Vertii et al. 2019). LAD regions correspond to around 40% of the genome and display heterochromatic characteristics and are relatively depleted of genes, which tend to be poorly transcribed. In plant cells, although no clear homologs of lamina have been found so far, plant-specific nuclear proteins CROWDED NUCLEI (CRWN) are thought to be lamina orthologs (Dittmer et al. 2007; Doğan and Liu 2018; Sakamoto and Takagi 2013). Plant mutated in *crwn* genes show an alteration of the CC nuclear distribution (Poulet et al. 2017). A first identification of LADs-like regions in plants has been performed using the NUCLEOPORIN 1 (NUP1) protein, located in the inner part of the nuclear pore complex (Bi et al. 2017). More recently, plant LADs (pLADs) have been identified using CRWN1 protein as a bait, by chromatin immunoprecipitation (Hu et al. 2019a). Pattern analyses of pLADs confirmed the enrichment of genomic domains displaying heterochromatic features (Bi et al. 2017; Hu et al. 2019a). How genes are silenced at the nuclear periphery remains an open question, but the fact that CRWN1 interacts with the protein PWWP INTERACTOR OF

POLYCOMB 1 (PWO1), a partner of the polycomb-group proteins (PcGs), suggest the involvement of PcGs in pLAD-gene silencing (Mikulski et al. 2019).

The largest nuclear compartment is the nucleolus, the site of ribosome biogenesis. Due to its high content in proteins, mainly implicated in the ribosome biogenesis pathway (Montacié et al. 2017; Sáez-Vásquez and Delseny 2019; Weis et al. 2015), the nucleolus is a very dense nuclear compartment, thought to contain only low amounts of the genomic sequences. However, in human cells, identification of nucleolus-associated chromatin domains (NADs) demonstrated that all 23 chromosomes possess at least a portion at the nucleolar periphery (van Köningsbruggen et al. 2010; Németh et al. 2010). Like LADs, NADs are mainly composed by large genomic regions displaying heterochromatic features. Interestingly, there is some overlap between LADs and NADs in human cells (Kind et al. 2013). A recent report was able separate two classes of NADs. “Type I NADs” are more heterochromatic and share domains with LADs. In contrast, “type II NADs” tend to be more prone to gene expression and enriched with developmentally regulated genes (Vertii et al. 2019). Microscopic observations suggest that interchangeable NADs and LADs are reshuffled after mitosis (Kind et al. 2013).

Using a technique enabling to isolate pure nucleoli directly from plant tissues, NADs were identified in *A. thaliana* (Pontvianne et al. 2016a, 2016b). As in mammalian cells, NADs *in A. thaliana* are enriched in genomic regions displaying repressive chromatin marks. Short arm of the chromosome 4 is by far the most enriched in *A. thaliana* (Pontvianne et al. 2016b). This chromosomic region has the particularity of containing actively transcribed rRNA genes, whose expression requires their association with the nucleolus, their site of transcription by the RNA polymerase I (Pontvianne et al. 2013). Additional rRNA genes are present on chromosome 2, but kept silent by epigenetic repressive marks and are located outside the nucleolus area (Chandrasekhara et al. 2016; Pontvianne et al. 2013). However, in a mutant that is affected in rRNA genes transcriptional regulation and in which rRNA genes from both chromosomes 2 and 4 are expressed, NADs composition is enriched by large genomic domains from the short arm of chromosome 2 (Picart and Pontvianne 2017; Pontvianne et al. 2016b). This suggests that NADs composition is largely dependent on rRNA genes organization and expression, a hypothesis that was recently confirmed by studies in human cells (Picart-Picolo et al. 2019; Quinodoz et al. 2018).

In *A. thaliana*, telomeres cluster at the nucleolar periphery (Armstrong et al. 2001; Fransz et al. 2002). NADs identification confirmed the presence of 200 to 300 kb of subtelomeric regions

of each chromosome end in the nucleolus (Pontvianne et al. 2016b). The role of telomeric sequences in the nucleolus of *A. thaliana* is not known, but a loss of their nucleolar localization correlates with a decrease in their length (Pontvianne et al. 2016b).

In addition, NADs are also composed of several hundred genes that tend to be silent (Pontvianne et al. 2016b). Because the RNA polymerase II is absent from the nucleolar interior, one hypothesis is that the nucleolus could be a sequestering area to keep genes silent (Pontvianne et al. 2016b). Some of them are developmentally regulated genes and future studies will certainly reveal whether their association is lost when there are expressed.

A comparison of NADs and pLADs from *A. thaliana*, unlike in animal cells, did not revealed a significant overlap (Picart-Picolo et al. 2019). However, regios of the short arm of the chromosome 4 have also been identified as pLADs. One possible explanation is the link between the nucleolus and the nuclear periphery. Indeed, the CC of the chromosome 4 associates with both the nucleolus and the nuclear periphery, creating a physical and indirect link between the nucleolus and the nuclear periphery.

Chromosomal loops

Chromosomal loops, leading to contacts of distant genomic regions at their base are recognized to play an important role in gene regulation. Interestingly, the first plant loop described has been associated to one of the most exotic modes of gene regulation, namely paramutation (Hollick 2016; Louwers et al. 2009). The maize *b1* gene has two epialleles, *B-I* and *B'* (Arteaga-Vazquez et al. 2010; Louwers et al. 2009; McEachern and Lloyd 2012). They share an identical DNA sequence but exhibit differential expression, leading to a clearly distinguishable pigmentation phenotype of husks (leaves surrounding the corncob). Green husks can be observed when the lowly expressed *B'* epiallele is present, whereas plants carrying the highly expressed *B-I* show purple husks. If the two are crossed, the transcriptional state of the paramutagenic *B'* allele is transmitted to *B-I*, leading to its downregulation and green husks throughout a segregating F2 generation (Louwers et al. 2009). This difference in expression levels may be mainly due to their differential 3D folding properties. In *B',* a single loop between its transcription start site (*TSS*) and a repeat region 117 kb upstream has been detected, whereas *B-I* additionally has loops anchoring between the *TSS* and regions lying in-between the repeats and the *b1* gene. However, an association of differential 3D folding and transcriptional state seems to be tissue specific, thus other – yet unknown – factors may be involved in epiallele formation in other tissues (Louwers et al. 2009).

In *A. thaliana*, several genomic loops associated with gene regulation have been described since the introduction of 3C technologies in plants. Loops have been described for prominent genes, such as the *FLOWERING LOCUS C* (*FLC*) (Crevillén et al. 2013; Jegu et al. 2014). FLC is a key regulator of flowering, which is suppressed when FLC is expressed. FLC transcription is gradually inhibited during vernalization by a Polycomb complex, leading to flowering initiation (Alexandre and Hennig, 2008). When FLC is transcribed, a gene loop anchored 5' and 3' of FLC can be observed and this loop is abolished after vernalization (Crevillén et al. 2013). This abolishment may be induced by binding of BAF60, a subunit of the SWI/SNF remodeling complex (Jegu et al. 2014) and may lead to the transcription of an FLC-antisense transcript, which is involved in FLC silencing (Swiezewski et al. 2009). Similar to FLC, an involvement of BAF60 in loop abolishment has also been reported in other genes (Jégu et al. 2015, 2017), however, whether BAF60 generally is involved in loop abolishment and subsequent gene silencing is questionable as chromatin binding profiles of BAF60 could generally be associated with active transcription (Jégu et al. 2017). FLC is not only regulated by a gene loop but also is involved in loop formation of its targets. Binding of FLC to the 3' regulatory region of *TARGET OF FLC AND SVP1* (*TFS1*) was reported to enable the formation of a gene loop anchoring at this 3' region and the *TFS1* gene body and promote *TFS1* silencing (Richter et al. 2019).

For *WUSCHEL,* another prominent *A. thaliana* gene, an association of gene looping with its transcriptional control has been reported (Guo et al. 2018). In case of *WUSCHEL*, the gene loop formed between its *TSS* and 3' flanking region is associated with *WUSCHEL* repression. Guo and colleagues studied the contribution of the loop anchor sequences and reported that neither the exact sequence nor distance between anchors is necessary for loop formation (Guo et al. 2018).

Gene loops are wide-spread features of *A. thaliana* 3D genome folding and additional loops have been identified by both 3C (Ariel et al. 2014; Cao et al. 2014; Liu et al. 2013; Wang et al. 2019) and Hi-C experiments (Liu et al. 2016). Generally, gene loops are associated with elevated transcription levels, not only in *A. thaliana* (Liu et al. 2016) but also in rice (Dong et al. 2018) and maize (Li et al. 2019) and, thus a positive correlation between gene looping and transcriptional activity may be a general feature in flowering plants.

Using chromatin interaction analysis by paired-end tag sequencing (ChIA-PET) for the first time in plants, two independent studies described numerous loops in maize (Li et al. 2019; Peng et al. 2019). These loops can be established between loci of similar epigenetic and transcriptional

state and, interestingly, between expression quantitative trait loci (eQTL) and their target genes (Peng et al. 2019). Additionally, long-range (up to 1 Mb) enhancer-promoter contacts were described that are associated with tissue-specific gene expression (Li et al. 2019). This may indicate that long-range contacts are rather part of a more complex and specialized regulatory machinery as opposed to short-range gene loops, which might be a hallmark of general gene regulation.

Despite the large number of known chromatin loops described in plants, their functional relevance remains largely elusive. Studying the exact biological role of chromatin loops is extremely difficult. As of today, our knowledge on factors mediating chromatin loops is scarce and one of the few ways available to analyze loops is to manipulate their anchor sequences. However, by doing so, there is always the risk that binding sites of important regulators may have been compromised. Thus, it is challenging to discriminate effects of loop abolishment and a potential lack of regulatory proteins.

The existence of thousands of gene loops in *A. thaliana* may compensate for the apparent absence of TADs. Gene loops may serve to insulate gene regulatory regions, similar as it is anticipated for animal TADs. In *A. thaliana,* transcriptional and epigenetic states of neighboring genes can widely differ, hence, making it more favorable to insulate single genes including their regulatory regions instead of insulating clusters of genes with similar transcriptional state as observed in animals (Szabo et al. 2019).

KNOT-linked silencing – a 3D silencing phenomenon

One of the most prominent features of *A. thaliana* 3D genome architecture is the *KNOT*, a 3D genomic structure formed by tight long-range *cis* and *trans* contacts among ten *KNOT engaged elements* (*KEEs*) (aka Interactive Heterochromatic Islands (IHIs))(Feng et al. 2014; Grob et al. 2014), which are distributed over all five *A. thaliana* chromosomes. High-frequency contacts among *KEEs* can be readily detected in Hi-C maps as they clearly stand out from contact frequencies observed between regions surrounding *KEEs*. *KEEs* are enriched in transposable elements (TEs) and associated small RNAs (sRNAs) (Grob et al., 2014) and exhibit a moderately heterochromatic constitution (Feng et al. 2014). However, their occurrence appears to be independent of a larger epigenetic context, as *KEEs* can be found in euchromatic regions of chromosome arms as well as constitutive heterochromatin of pericentromeres. TEs found within *KEEs* are significantly enriched in fragments of *VANDAL6* DNA transposons and potentially full-length *ATLANTYS3* retrotransposons (Dong et al. 2018; Grob and Grossniklaus

2017; Grob et al. 2014). Furthermore, the *KNOT* is likely conserved, both in structure and sequences, as high-frequency contacts between TE islands can also be detected in rice (Dong et al. 2018).

Factors involved in the *KEE-KEE* contact and *KNOT* formation have not been identified to date, despite the various mutants that have been screened by Hi-C in *A. thaliana* (Feng et al. 2014; Grob et al. 2014). Interestingly, the *KNOT* is not abolished in various mutant affecting epigenetic pathways:

Histone H3 lysine 9 di-methylation (H3K9me2) is an important repressive epigenetic mark and enriched in heterochromatin and is impaired in su(var)3-9 homolog 4 (suvh4) suvh5 suvh6 triple mutants. However, despite slight enrichment of H3K9me2 in *KEEs*, *KNOT* formation is not impaired in the suvh4 suvh5 suvh6 triple mutants (Feng et al. 2014). Similarly, DNA methylation mutants *decreased in DNA methylation* 1 (*ddm1*), *methyltransferase 1* (*met1*), and *chromomethylase 3* (*cmt3*) do not lead to *KNOT* abolishment. Moreover, in *ddm1* and *met1* mutants, ten additional *KEEs* can be found, which completely overlap between the two mutants. Interestingly, three additional *KEEs* can also be observed in H3K9me2 mutants and two of them overlap with those found in the *met1* and *ddm1* mutants (Feng et al. 2014). Additional *KEEs* do not appear to emerge from random positions, as ectopic *KEEs* are also enriched in *VANDAL6* TE fragments. Mutations in other suspects, such as the Polycomb gene *curly leaf* (*clf*) and *swinger* (*swn*) and chromatin remodelers *microchidia 6* (*morc6*) and *morpheus molecule 1* (*mom1*) do also not negatively affect the *KNOT* (Feng et al. 2014).

Despite the scarce knowledge on how the *KNOT* is formed, more is known about its biological function. DNA transposons have been shown to preferentially insert into *KEEs* (Grob et al. 2014), leading to the speculation that *KEEs* could be involved in TE biology. This hypothesis has been supported by the finding of a novel silencing phenomenon, termed *KNOT-linked silencing* (KLS) (Grob and Grossniklaus 2019): The insertion site of T-DNA transgenes can form ectopic contacts with single *KEEs* or the entire *KNOT* and these ectopic contact correlate to the transgene's expression state. Transgenes that form ectopic contacts with the entire *KNOT* are fully silenced, whereas transgenes exhibiting ectopic contacts to a single *KEE* only are stably expressed, similar to transgenes that do not form ectopic *KEE* contacts at all. RNA-dependent DNA methylation (RdDM) and sRNA-induced post-transcriptional gene silencing are not involved in KLS, leading to speculations whether KLS represents a completely novel silencing mechanism. The differential pattern observed in KLS by active transgenic lines that

show only ectopic contacts to single *KEEs* and repressed lines that exhibit full *KNOT* association is of special interest: the study of KLS offers the rare opportunity to investigate both transgene detection (single *KEE* contacts) and subsequent transgene silencing (full *KNOT* association).

Conclusions

The study of nuclear architecture gained increasing attention in recent years. With the establishment of novel technologies, we are today not only able to characterize contact frequencies among genomic regions, but we can also locate these regions in relation to important nuclear compartments. As Hi-C became a favorite tool to support genome assemblies, Hi-C data sets for various plant species are available to date. However, many of them seem to be byproducts of assemblies and not all of them suffice in quality for in-depth analysis. Thus, *A. thaliana* still represents the best-studied model concerning nuclear architecture in plants. Further studies in other species, including the characterization of LADs and NADs could shed more light on plant nuclear architecture, especially since nuclear architecture in *A. thaliana* may be rather exceptional among plants.

Acknowledgments

FP is supported by CNRS, the ANR JCJC NucleoReg [ANR-15-CE12-0013-01] and the French Laboratory of Excellence project TULIP (ANR-10-LABX-41 and ANR-11-IDEX-0002-02). SG is supported by the University of Zurich.

References

Alexandre, C.M., and Hennig, L. (2008). FLC or not FLC: the other side of vernalization. J. Exp. Bot. *59*, 1127–1135.

Alipour, E., and Marko, J.F. (2012). Self-organization of domain structures by DNA-loop-extruding enzymes. Nucleic Acids Res. *40*, 11202–11212.

Andrey, P., Kiêu, K., Kress, C., Lehmann, G., Tirichine, L., Liu, Z., Biot, E., Adenot, P.G., Hue-Beauvais, C., Houba-Hérin, N., et al. (2010). Statistical analysis of 3D images detects regular spatial distributions of centromeres and chromocenters in animal and plant nuclei. PLoS Comput. Biol. *6*, 27.

Ariel, F., Jegu, T., Latrasse, D., Romero-Barrios, N., Christ, A., Benhamed, M., and Crespi, M. (2014). Noncoding transcription by alternative RNA polymerases dynamically regulates an auxin-driven chromatin loop. Mol. Cell *55*, 383–396.

Armstrong, S.J., Franklin, F.C., and Jones, G.H. (2001). Nucleolus-associated telomere clustering and pairing precede meiotic chromosome synapsis in *Arabidopsis thaliana*. J. Cell Sci. *114*, 4207–4217.

Arteaga-Vazquez, M., Sidorenko, L., Rabanal, F.A., Shrivistava, R., Nobuta, K., Green, P.J., Meyers, B.C., and Chandler, V.L. (2010). RNA-mediated *trans*-communication can establish paramutation at the *b1* locus in maize. Proc. Natl. Acad. Sci. *107*, 12986–12991.

Barneche, F., Malapeira, J., and Paloma, M. (2014). The impact of chromatin dynamics on plant light responses and circadian clock function. J. Exp. Bot. *65*, 2895–2913.

Bi, X., Cheng, Y., Hu, B., Ma, X., Wu, R., and Wang, J. (2017). Nonrandom domain organization of the *Arabidopsis* genome at the nuclear periphery. Genome Res. *27*, 1162–1173.

Bonev, B., and Cavalli, G. (2016). Organization and function of the 3D genome. Nat. Rev. Genet. *17*, 772.

Cao, S., Kumimoto, R.W., Gnesutta, N., Calogero, A.M., Mantovani, R., and Holt, B.F. (2014). A distal CCAAT/NUCLEAR FACTOR Y complex promotes chromatin looping at the *FLOWERING LOCUS T* promoter and regulates the timing of flowering in *Arabidopsis*. Plant Cell *26*, 1009–1017.

Chandrasekhara, C., Mohannath, G., Blevins, T., Pontvianne, F., and Pikaard, C.S. (2016). Chromosome-specific NOR inactivation explains selective rRNA gene silencing and dosage control in *Arabidopsis*. Genes Dev. *30*, 177–190.

Cook, P.R., and Marenduzzo, D. (2018). Transcription-driven genome organization: a model for chromosome structure and the regulation of gene expression tested through simulations. Nucleic Acids Res. *46*, 9895–9906.

Cremer, T., and Cremer, C. (2001). Chromosome territories, nuclear architecture and gene regulation in mammalian cells. Nat. Rev. Genet. *2*, 292–301.

Crevillén, P., Sonmez, C., Wu, Z., and Dean, C. (2013). A gene loop containing the floral repressor FLC is disrupted in the early phase of vernalization. EMBO J. *32*, 140–148.

Dekker, J., Rippe, K., Dekker, M., and Kleckner, N. (2002). Capturing chromosome conformation. Science. *295*, 1306–1311.

Dittmer, T.A., Stacey, N.J., Sugimoto-Shirasu, K., and Richards, E.J. (2007). *LITTLE NUCLEI* genes affecting nuclear morphology in *Arabidopsis thaliana*. Plant Cell *19*, 2793–2803.

Doğan, E.S., and Liu, C. (2018). Three-dimensional chromatin packing and positioning of plant genomes. Nat. Plants *4*, 521–529.

Dong, P., Tu, X., Chu, P., Peitao, L., Zhu, N., Grierson, D., Du, B., Li, P., and Zhong, S. (2017). 3D chromatin architecture of large plant genomes determined by local A/B compartments. Mol. Plant *10*, 1497–1509.

Dong, P., Tu, X., Li, H., Zhang, J., Grierson, D., Li, P., and Zhong, S. (2019). Tissue-specific Hi-C analyses of rice, foxtail millet and maize suggest non-canonical function of plant chromatin domains. J. Integr. Plant Biol.

Dong, Q., Li, N., Li, X., Yuan, Z., Xie, D., Wang, X., Li, J., Yu, Y., Wang, J., Ding, B., et al. (2018). Genome-wide Hi-C analysis reveals extensive hierarchical chromatin interactions in rice. Plant J. *94*, 1141–1156.

Fang, Y., and Spector, D.L. (2005). Centromere positioning and dynamics in living *Arabidopsis* plants. Mol. Biol. Cell *16*, 5710–5718.

Feng, S., Cokus, S.J., Schubert, V., Zhai, J., Pellegrini, M., and Jacobsen, S.E. (2014). Genome-wide Hi-C analyses in wild-type and mutants reveal high-resolution chromatin interactions in *Arabidopsis*. Mol. Cell *55*, 694–707.

Fransz, P., De Jong, J.H., Lysak, M., Castiglione, M.R., and Schubert, I. (2002). Interphase chromosomes in *Arabidopsis* are organized as well defined chromocenters from which euchromatin loops emanate. Proc. Natl. Acad. Sci. U. S. A. *99*, 14584–14589.

Grob, S. (2019). Three-dimensional chromosome organization in flowering plants. Brief. Funct. Genomics. elz024.

Grob, S., and Grossniklaus, U. (2017). Chromosome conformation capture-based studies reveal novel features of plant nuclear architecture. Curr. Opin. Plant Biol. *36*, 149–157.

Grob, S., and Grossniklaus, U. (2019). Invasive DNA elements modify the nuclear architecture of their insertion site by *KNOT* - linked silencing in *Arabidopsis thaliana*. Genome Biol. *20*, 120.

Grob, S., Schmid, M.W., Luedtke, N.W., Wicker, T., and Grossniklaus, U. (2013). Characterization of chromosomal architecture in *Arabidopsis* by chromosome conformation capture. Genome Biol. *14*, R129.

Grob, S., Schmid, M.W., and Grossniklaus, U. (2014). Hi-C analysis in *Arabidopsis* identifies the KNOT, a structure with similarities to the flamenco locus of Drosophila. Mol. Cell *55*, 678–693.

Guelen, L., Pagie, L., Brasset, E., Meuleman, W., Faza, M.B., Talhout, W., Eussen, B.H., de Klein, A., Wessels, L., De Laat, W., et al. (2008). Domain organization of human chromosomes revealed by mapping of nuclear lamina interactions. Nature *453*, 948–951.

Guo, L., Cao, X., Liu, Y., Li, J., Li, Y., Li, D., Zhang, K., Gao, C., Dong, A., and Liu, X. (2018). A chromatin loop represses *WUSCHEL* expression in *Arabidopsis*. Plant J. *94*, 1083–1097.

Guo, Y., Xu, Q., Canzio, D., Krainer, A.R., Maniatis, T., Guo, Y., Xu, Q., Canzio, D., Shou, J., Li, J., et al. (2015). CRISPR inversion of CTCF sites alters genome topology and enhancer/promoter function. Cell *162*, 900–910.

Heitz, E. (1928). Das Heterochromatin der Moose. Jahrbücher Für Wissenschaftliche Bot. *69*, 762–818.

Hollick, J.B. (2016). Paramutation and related phenomena in diverse species. Nat. Rev. Genet. *18*, 5–23.

Hu, B., Wang, N., Bi, X., Karaaslan, E.S., Weber, A., Zhu, W., Berendzen, K.W., and Liu, C. (2019a). Plant lamin-like proteins mediate chromatin tethering at the nuclear periphery. Genome Biol. *20*.

Hu, L., Xu, Z., Wang, M., Fan, R., Yuan, D., Wu, B., Wu, H., Qin, X., Yan, L., Tan, L., et al. (2019b). The chromosome-scale reference genome of black pepper provides insight into piperine biosynthesis. Nat. Commun. *10*, 4702.

Hu, Y., Chen, J., Fang, L., Zhang, Z., Ma, W., Niu, Y., Ju, L., Deng, J., Zhao, T., Lian, J., et al. (2019c). *Gossypium barbadense* and *Gossypium hirsutum* genomes provide insights into the origin and evolution of allotetraploid cotton. Nat. Genet. *51*, 739–748.

Jegu, T., Latrasse, D., Delarue, M., Hirt, H., Domenichini, S., Ariel, F., Crespi, M., Bergounioux, C., Raynaud, C., and Benhamed, M. (2014). The BAF60 subunit of the SWI/SNF chromatin-remodeling complex directly controls the formation of a gene loop at *FLOWERING LOCUS C* in *Arabidopsis*. Plant Cell *26*, 538–551.

Jégu, T., Domenichini, S., Blein, T., Ariel, F., Christ, A., Kim, S., Crespi, M., Boutet-Mercey, S., Mouille, G., Bourge, M., et al. (2015). A SWI/SNF chromatin remodelling protein controls cytokinin production through the regulation of chromatin architecture. PLoS One *10*, e0138276.

Jégu, T., Veluchamy, A., Ramirez-prado, J.S., Rizzi-paillet, C., Perez, M., Lhomme, A., Latrasse, D., Coleno, E., Vicaire, S., Legras, S., et al. (2017). The *Arabidopsis* SWI/SNF protein BAF60 mediates seedling growth control by modulating DNA accessibility. Genome Biol. *18*, 1–16.

Jibran, R., Dzierzon, H., Bassil, N., Bushakra, J.M., Edger, P.P., Sullivan, S., Finn, C.E., Dossett, M., Vining, K.J., Vanburen, R., et al. (2018). Chromosome-scale scaffolding of the black raspberry (*Rubus occidentalis L.*) genome based on chromatin interaction data. Hortic. Res. *5*.

Kaiserli, E., Pa, K., Donnell, L.O., Nusinow, D.A., Kay, S.A., Chory, J., Donnell, L.O., Batalov, O., Pedmale, U. V, Nusinow, D.A., et al. (2015). Integration of light and photoperiodic signaling in transcriptional nuclear foci. Dev. Cell 311–321.

Kind, J., Pagie, L., Ortabozkoyun, H., Boyle, S., de Vries, S.S., Janssen, H., Amendola, M., Nolen, L.D., Bickmore, W.A., and van Steensel, B. (2013). Single-cell dynamics of genome-nuclear lamina interactions. Cell *153*, 178–192.

van Königsbruggen, S., Gierliński, M., Schofield, P., Martin, D., Barton, G.J., Ariyurek, Y., den Dunnen, J.T., and Lamond, A.I. (2010). High-resolution whole-genome sequencing reveals that specific chromatin domains from most human chromosomes associate with nucleoli. Mol. Biol. Cell *21*, 3735–3748.

Lamesch, P., Berardini, T.Z., Li, D., Swarbreck, D., Wilks, C., Sasidharan, R., Muller, R., Dreher, K., Alexander, D.L., Garcia-hernandez, M., et al. (2012). The *Arabidopsis* Information Resource (TAIR): improved gene annotation and new tools. Nucleic Acids Res. *40*, 1202–1210.

Li, E., Liu, H., Huang, L., Zhang, X., Dong, X., Song, W., Zhao, H., and Lai, J. (2019). Long-range interactions between proximal and distal regulatory regions in maize. Nat. Commun. *10*, 2633.

Lieberman-Aiden, E., Van Berkum, N.L., Williams, L., Imakaev, M., Ragoczy, T., Telling, A., Amit, I., Lajoie, B.R., Sabo, P.J., Dorschner, M.O., et al. (2009). Comprehensive mapping of long-range interactions reveals folding principles of the human genome. Science. *326*, 289–293.

Lister, R., O'Malley, R.C., Tonti-Filippini, J., Gregory, B.D., Berry, C.C., Millar, A.H., and Ecker, J.R. (2008). Highly integrated single-base resolution maps of the epigenome in *Arabidopsis*. Cell *133*, 523–536.

Liu, C., Teo, Z.W.N., Bi, Y., Song, S., Xi, W., Yang, X., Yin, Z., and Yu, H. (2013). A conserved genetic pathway determines inflorescence architecture in arabidopsis and rice. Dev. Cell *24*, 612–622.

Liu, C., Wang, C., Wang, G., Becker, C., Zaidem, M., and Weigel, D. (2016). Genome-wide

analysis of chromatin packing in *Arabidopsis thaliana* at single-gene resolution. Genome Res. *26*, 1057–1068.

Liu, C., Cheng, Y.-J., Wang, J.-W., and Weigel, D. (2017). Prominent topologically associated domains differentiate global chromatin packing in rice from *Arabidopsis*. Nat. Plants *3*, 742–748.

Louwers, M., Bader, R., Haring, M., Van Driel, R., De Laat, W., and Stam, M. (2009). Tissue- and expression level-specific chromatin looping at maize b1 epialleles. Plant Cell *21*, 832–842.

Maccaferri, M., Harris, N.S., Twardziok, S.O., Pasam, R.K., Gundlach, H., Spannagl, M., Ormanbekova, D., Lux, T., Prade, V.M., Milner, S.G., et al. (2019). Durum wheat genome highlights past domestication signatures and future improvement targets. Nat. Genet. *51*, 885–895.

Mascher, M., Gundlach, H., Himmelbach, A., Beier, S., Twardziok, S.O., Wicker, T., Radchuk, V., Dockter, C., Hedley, P.E., Russell, J., et al. (2017). A chromosome conformation capture ordered sequence of the barley genome. Nature *544*, 427–433.

McEachern, L.A., and Lloyd, V.K. (2012). The maize b1 paramutation control region causes epigenetic silencing in *Drosophila melanogaster*. Mol. Genet. Genomics *287*, 591–606.

Mikulski, P., Hohenstatt, M.L., Farrona, S., Smaczniak, C., Stahl, Y., Kalyanikrishna, Kaufmann, K., Angenent, G., and Schubert, D. (2019). The chromatin-associated protein PWO1 interacts with plant nuclear lamin-like components to regulate nuclear size. Plant Cell *31*, 1141 LP – 1154.

Moissiard, G., Cokus, S.J., Cary, J., Feng, S., Billi, A.C., Stroud, H., Husmann, D., Zhan, Y., Lajoie, B.R., McCord, R.P., et al. (2012). MORC family ATPases required for heterochromatin condensation and gene silencing. Science. *336*, 1448–1451.

Montacié, C., Durut, N., Opsomer, A., Palm, D., Comella, P., Picart, C., Carpentier, M.-C., Pontvianne, F., Carapito, C., Schleiff, E., et al. (2017). Nucleolar proteome analysis and proteasomal activity assays reveal a link between nucleolus and 26S proteasome in *A. thaliana*. Front. Plant Sci. *8*, 1815.

Németh, A., Conesa, A., Santoyo-Lopez, J., Medina, I., Montaner, D., Péterfia, B., Solovei, I., Cremer, T., Dopazo, J., and Längst, G. (2010). Initial genomics of the human nucleolus. PLOS Genet. *6*, 1–11.

Pavet, V., Quintero, C., Cecchini, N.M., Rosa, A.L., and Alvarez, M.E. (2006). *Arabidopsis* displays centromeric dna hypomethylation and cytological alterations of heterochromatin upon attack by *Pseudomonas syringae*. Mol. Plant-Microbe Interact. *19*, 577–587.

Pecinka, A., Schubert, V., Meister, A., Kreth, G., Klatte, M., Lysak, M.A., Fuchs, J. rg, and Schubert, I. (2004). Chromosome territory arrangement and homologous pairing in nuclei of *Arabidopsis thaliana* are predominantly random except for NOR-bearing chromosomes. Chromosoma *113*, 258–269.

Pecinka, A., Dinh, H.Q., Baubec, T., Rosa, M., Lettner, N., and Scheid, O.M. (2010). Epigenetic regulation of repetitive elements is attenuated by prolonged heat stress in *Arabidopsis*. Plant Cell *22*, 3118–3129.

Peng, Y., Xiong, D., Zhao, L., Ouyang, W., Wang, S., Sun, J., Zhang, Q., Guan, P., Xie, L., Li, W., et al. (2019). Chromatin interaction maps reveal genetic regulation for quantitative traits in

582 maize. Nat. Commun. *10*, 2632.

583 Phillips, J.E., and Corces, V.G. (2009). CTCF : Master weaver of the genome. Cell *137*, 1194–
584 1211.

585 Picart-Picolo, A., Picault, N., and Pontvianne, F. (2019). Ribosomal RNA genes shape
586 chromatin domains associating with the nucleolus. Nucleus *10*, 67–72.

587 Picart, C., and Pontvianne, F. (2017). Plant nucleolar DNA: Green light shed on the role of
588 Nucleolin in genome organization. Nucleus *8*, 11–16.

589 Pickersgill, H., Kalverda, B., de Wit, E., Talhout, W., Fornerod, M., and van Steensel, B.
590 (2006). Characterization of the *Drosophila melanogaster* genome at the nuclear lamina. Nat.
591 Genet. *38*, 1005–1014.

592 Pontvianne, F., Blevins, T., Hassel, C., Pontes, O.M.F., Muchova, V., Tucker, S., Mokros, P.,
593 Muchova, V., Fajkus, J., and Pikaard, C.S. (2013). Subnuclear partitioning of rRNA genes
594 between the nucleolus and nucleoplasm reflects alternative epiallelic states. Genes Dev. *27*,
595 1545–1550.

596 Pontvianne, F., Boyer-Clavel, M., and Sáez-Vásquez, J. (2016a). Fluorescence-activated
597 nucleolus sorting in *Arabidopsis*. In: Németh A (ed) The nucleolus: methods and protocols.
598 Springer New York, New York, pp 203–211.

599 Pontvianne, F., Carpentier, M.C., Durut, N., Pavlištová, V., Jaške, K., Schořová, Š., Parrinello,
600 H., Rohmer, M., Pikaard, C.S., Fojtová, M., et al. (2016b). Identification of nucleolus-
601 associated chromatin domains reveals a role for the nucleolus in 3D organization of the
602 *A. thaliana* genome. Cell Rep. *16*, 1574–1587.

603 Poulet, A., Duc, C., Voisin, M., Desset, S., Tutois, S., Vanrobays, E., Benoit, M., Evans, D.E.,
604 Probst, A. V, and Tatout, C. (2017). The LINC complex contributes to heterochromatin
605 organisation and transcriptional gene silencing in plants. J. Cell Sci. *130*, 590 LP – 601.

606 Quinodoz, S.A., Ollikainen, N., Tabak, B., Palla, A., Schmidt, J.M., Detmar, E., Lai, M.M.,
607 Shishkin, A.A., Bhat, P., Takei, Y., et al. (2018). Higher-Order Inter-chromosomal hubs shape
608 3D genome organization in the nucleus. Cell *174*, 744-757.e24.

609 Rada-Iglesias, A., Grosveld, F.G., and Papantonis, A. (2018). Forces driving the three-
610 dimensional folding of eukaryotic genomes. Mol. Syst. Biol. *14*, e8214.

611 Raymond, O., Gouzy, J., Just, J., Badouin, H., Verdenaud, M., Lemainque, A., Vergne, P.,
612 Moja, S., Choisne, N., Pont, C., et al. (2018). The Rosa genome provides new insights into the
613 domestication of modern roses. Nat. Genet. *50*, 772–777.

614 Richter, R., Kinoshita, A., Vincent, C., Martinez-Gallegos, R., Gao, H., van Driel, A.D., Hyun, Y.,
615 Mateos, J.L., and Coupland, G. (2019). Floral regulators FLC and SOC1 directly regulate
616 expression of the B3-type transcription factor *TARGET OF FLC AND SVP 1* at the *Arabidopsis*
617 shoot apex via antagonistic chromatin modifications. PLoS Genet. *15*, e1008065.

618 Rowley, M.J., and Corces, V.G. (2018). Organizational principles of 3D genome architecture.
619 Nat. Rev. Genet. *19*, 789–800.

620 Rowley, M.J., Nichols, M.H., Lyu, X., Ando-Kuri, M., Riviera, S.M., Hermetz, K., Wang, P.,
621 Ruan, Y., and Corces, V.G. (2017). Evolutionarily conserved principles predict 3D chromatin
622 organization. Mol. Cell *67*, 837-852.e7.

623 Sáez-Vásquez, J., and Delseny, M. (2019). Ribosome biogenesis in plants: from functional 45S

ribosomal DNA organization to ribosome assembly factors. Plant Cell *31*, 1945 LP – 1967.

Sakamoto, Y., and Takagi, S. (2013). LITTLE NUCLEI 1 and 4 regulate nuclear morphology in *Arabidopsis thaliana*. Plant Cell Physiol. *54*, 622–633.

Sanborn, A.L., Rao, S.S.P., Huang, S., Durand, N.C., Huntley, M.H., Jewett, A.I., Bochkow, I.D., Chinnappan, D., Cutkosky, A., Jian, L., et al. (2015). Chromatin extrusion explains key features of loop and domain formation in wild-type and engineered genomes. Proc. Natl. Acad. Sci. U. S. A. *112*, E6456–E6465.

Santos, A.P., and Shaw, P. (2004). Interphase chromosomes and the Rabl configuration: does genome size matter? J. Microsc. *214*, 201–206.

dos Santos, G., Schroeder, A.J., Goodman, J.L., Strelets, V.B., Crosby, M.A., Thurmond, J., Emmert, D.B., Gelbart, W.M., and Consortium, F. (2015). FlyBase: introduction of the Drosophila melanogaster Release 6 reference genome assembly and large-scale migration of genome annotations. Nucleic Acids Res. *43*, D690–D697.

Schubert, V., Weißleder, A., Ali, H., Fuchs, J., Lermontova, I., Meister, A., and Schubert, I. (2009). Cohesin gene defects may impair sister chromatid alignment and genome stability in *Arabidopsis thaliana*. Chromosoma *118*, 591–605.

Schwarzer, W., Abdennur, N., Goloborodko, A., Pekowska, A., Fudenberg, G., Loe-mie, Y., Fonseca, N.A., Huber, W., Haering, C.H., Mirny, L., et al. (2017). Two independent modes of chromatin organization revealed by cohesin removal. Nature *551*, 51–56.

Sexton, T., and Cavalli, G. (2015). The role of chromosome domains in shaping the functional genome. Cell *160*, 1049–1059.

Sexton, T., Yaffe, E., Kenigsberg, E., Bantignies, F., Leblanc, B., Hoichman, M., Parrinello, H., Tanay, A., and Cavalli, G. (2012). Three-dimensional folding and functional organization principles of the *Drosophila* genome. Cell *148*, 458–472.

Shi, J., Ma, X., Zhang, J., Zhou, Y., Liu, M., Huang, L., Sun, S., Zhang, X., Gao, X., Zhan, W., et al. (2019) Chromosome conformation capture resolved near complete genome assembly of broomcorn millet. Nat. Commun. *10*, 464.

Sotelo-Silveira, M., Chávez Montes, R.A., Sotelo-Silveira, J.R., Marsch-Martínez, N., and de Folter, S. (2018). Entering the next dimension: plant genomes in 3D. Trends Plant Sci. *23*, 598–612.

Stam, M., Tark-dame, M., and Fransz, P. (2019). 3D genome organization : a role for phase separation and loop extrusion ? Curr. Opin. Plant Biol. *48*, 36–46.

Strom, A.R., Emelyanov, A. V, Mir, M., Fyodorov, D. V, Darzacq, X., and Karpen, G.H. (2017). Phase separation drives heterochromatin domain formation. Nature *547*, 241–245.

Stroud, H., Do, T., Du, J., Zhong, X., Feng, S., Johnson, L., Patel, D.J., and Jacobsen, S.E. (2014). Non-CG methylation patterns shape the epigenetic landscape in *Arabidopsis*. Nat. Struct. Mol. Biol. *21*, 64–72.

Swiezewski, S., Liu, F., Magusin, A., and Dean, C. (2009). Cold-induced silencing by long antisense transcripts of an *Arabidopsis* Polycomb target. Nature *462*, 799–802.

Szabo, Q., Jost, D., Chang, J., Cattoni, D.I., Papadopoulos, G.L., Bonev, B., Sexton, T., Gurgo, J., Jacquier, C., Nollmann, M., et al. (2018). TADs are 3D structural units of higher-order chromosome organization in *Drosophila*. Sci. Adv. *4*, eaar8082.

Szabo, Q., Bantignies, F., and Cavalli, G. (2019). Principles of genome folding into topologically associating domains. Sci. Adv. *5*, eaaw1668.

Tessadori, F., Schulkes, R.K., Driel, R. Van, and Fransz, P. (2007). Light-regulated large-scale reorganization of chromatin during the floral transition in *Arabidopsis*. Plant J. *2*, 848–857.

VanBuren, R., Wai, C.M., Pardo, J., Giarola, V., Ambrosini, S., Song, X., and Bartels, D. (2018). Desiccation tolerance evolved through gene duplication and network rewiring in *Lindernia*. Plant Cell *30*, 2943–2958.

Vertii, A., Ou, J., Yu, J., Yan, A., Pagès, H., Liu, H., and Zhu, L.J. (2019). Two contrasting classes of nucleolus-associated domains in mouse fibroblast heterochromatin. Genome Res. *29*, 1235–1249.

Wang, H., Li, S., Li, Y., Xu, Y., Wang, Y., Zhang, R., Sun, W., Chen, Q., Wang, X., Li, C., et al. (2019). MED25 connects enhancer–promoter looping and MYC2-dependent activation of jasmonate signalling. Nat. Plants *5*, 616–625.

Wang, M., Wang, P., Lin, M., Ye, Z., Li, G., Tu, L., Shen, C., Li, J., Yang, Q., and Zhang, X. (2018). Evolutionary dynamics of 3D genome architecture following polyploidization in cotton. Nat. Plants *4*, 90–97.

Weis, B.L., Kovacevic, J., Missbach, S., and Schleiff, E. (2015). Plant-specific features of ribosome biogenesis. Trends Plant Sci. *20*, 729–740.

Zhang, L., Cai, X., Wu, J., Liu, M., Grob, S., Cheng, F., Liang, J., Cai, C., Liu, Z., Liu, B., et al. (2018). Improved Brassica rapa reference genome by single-molecule sequencing and chromosome conformation capture technologies. Hortic. Res. *5*.

Zhang, X., Yazaki, J., Sundaresan, A., Cokus, S., Chan, S.W.-L., Chen, H., Henderson, I.R., Shinn, P., Pellegrini, M., Jacobsen, S.E., et al. (2006). Genome-wide high-resolution mapping and functional analysis of DNA methylation in *Arabidopsis*. Cell *126*, 1189–1201.

Zhu, W., Hu, B., Becker, C., Süheyla, E., and Berendzen, K.W. (2017). Altered chromatin compaction and histone methylation drive non-additive gene expression in an interspecific *Arabidopsis* hybrid. Genome Biol. *18*, 157.

Figure Legends

Fig. 1 The 3D genome is organized at multiple scales. For each scale, an illustration is given accompanied with typical features of Hi-C maps (adapted from Grob (2019)). LSD: Loose Structural Domain; CSD: Closed Structural Domain; CEN: Centromere; TAD: Topologically Associating Domain.

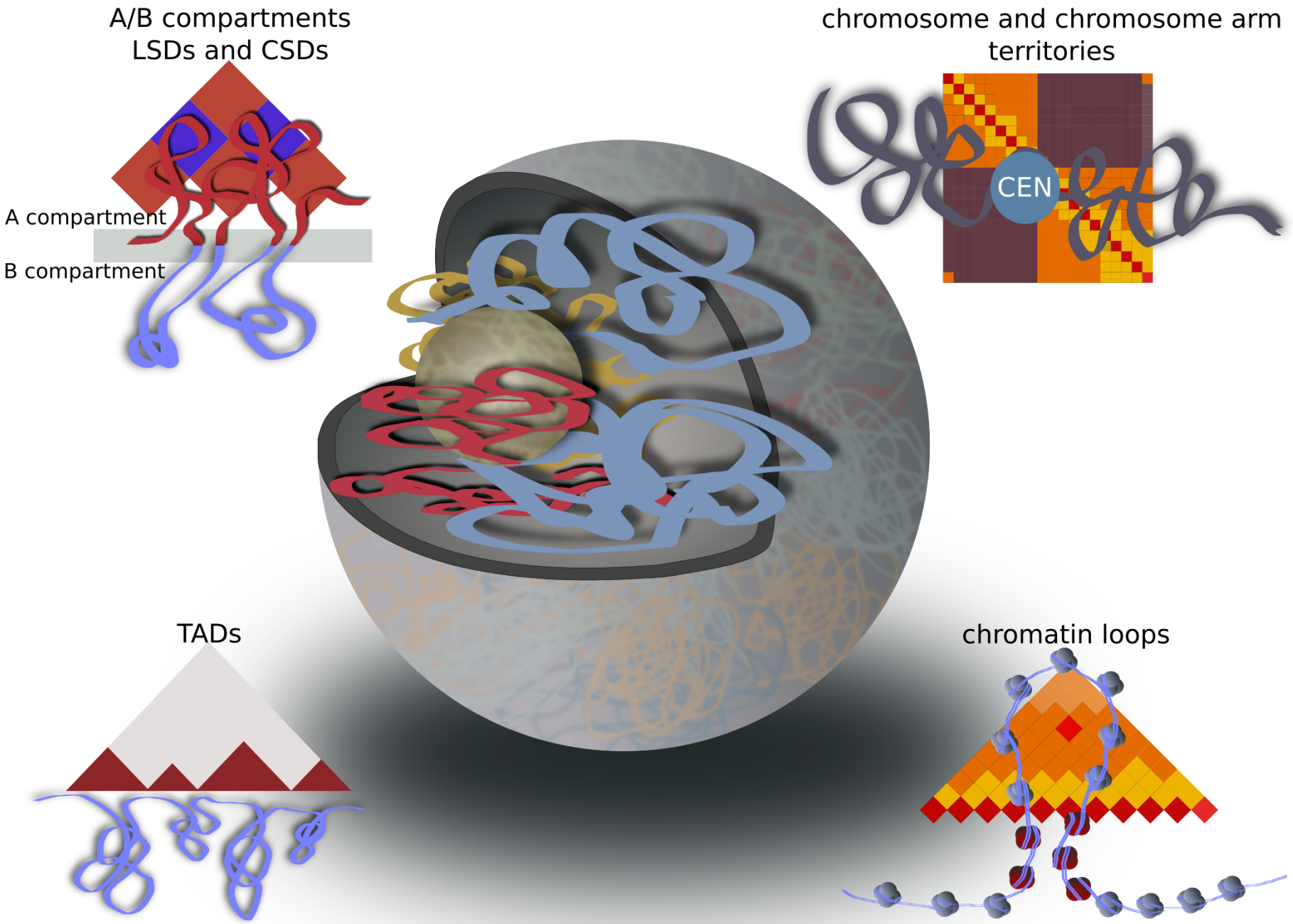
A/B compartments
LSDs and CSDs
A compartment
B compartment
chromosome and chromosome arm
territories
CEN
TADs
chromatin loops